Journal of Coordination Chemistry
Publication details, including instructions for authors and subscription information:
http://www.tandfonline.com/loi/gcoo20

Preparation of a fluorescent sensor based on BODIPY-functionalized hydroxyapatite nanoparticles and spectroscopic study of the Cd^{2+} and Zn^{2+} complex formation

Xu Jia [a], Xiaoting Yu [a], Guolin Zhang [a], Weisheng Liu [a] & Wenwu Qin [a]

[a] Key Laboratory of Nonferrous Metal Chemistry and Resources Utilization of Gansu Province and State Key Laboratory of Applied Organic Chemistry, College of Chemistry and Chemical Engineering, Lanzhou University, Lanzhou, 730000, P.R. China

Accepted author version posted online: 18 Jan 2013.Published online: 05 Mar 2013.

To cite this article: Xu Jia, Xiaoting Yu, Guolin Zhang, Weisheng Liu & Wenwu Qin (2013) Preparation of a fluorescent sensor based on BODIPY-functionalized hydroxyapatite nanoparticles and spectroscopic study of the Cd^{2+} and Zn^{2+} complex formation, Journal of Coordination Chemistry, 66:4, 662-670, DOI: 10.1080/00958972.2013.767896

To link to this article: http://dx.doi.org/10.1080/00958972.2013.767896

Journal of Coordination Chemistry
Vol. 66, No. 4, 20 February 2013, 662–670

Preparation of a fluorescent sensor based on BODIPY-functionalized hydroxyapatite nanoparticles and spectroscopic study of the Cd^{2+} and Zn^{2+} complex formation

XU JIA, XIAOTING YU, GUOLIN ZHANG, WEISHENG LIU and WENWU QIN*

Key Laboratory of Nonferrous Metal Chemistry and Resources Utilization of Gansu Province and State Key Laboratory of Applied Organic Chemistry, College of Chemistry and Chemical Engineering, Lanzhou University, Lanzhou 730000, P.R. China

(*Received 3 September 2012; in final form 14 November 2012*)

A new fluorescent chemosensor **1**, which based on hydroxyapatite (HA) nanoparticles covalently functionalized with a difluoroboron dipyrromethene, has been prepared by nucleophilic substitution of the fluorescent dye 3-chloro-4,4-difluoro-8-(4-tolyl)-5-[bis(pyridine2-ylmethyl)amino]-4-bora-3a,4a-diaza-*s*-indacene (**2**) with surface-modified HA nanoparticles. The HA particles were prepared by using SiO_2 as templates (THA) with 3-(aminopropyl)triethoxysilane (THA-APTES). Substitution of the electron-withdrawing chlorine in **2** by an electron-donating amino group of HA changes the properties of the nanoparticles **1** and the corresponding fluorescent dye **2**. Absorption and emission maxima of **1** in ethanol are red-shifted by 75 and 30 nm, respectively, in comparison with those of **2**. In contrast to no selectivity of dye **2** for Cd^{2+} or Zn^{2+} in EtOH/H_2O (95/5 V/V) solutions, the nanofluorescent probe **1** forms 1 : 1 complexes with Cd^{2+} or Zn^{2+}, producing an instant color change along with large *hypsochromic* shifts in the absorption and fluorescence spectra by 70 and 35 nm, respectively, and large cation-induced fluorescence amplifications.

Keywords: Hydroxyapatite (HA) nanoparticles; BODIPY-functionalized; Nanofluorescent sensor; Cadmium and zinc complex formation

1. Introduction

The design, synthesis, and spectroscopic/photophysical characterization of fluorescent chemosensors continue to be topics of research [1,2]. Derivatives of 4,4-difluoro-4-bora-3a,4adiaza-*s*-indacene [3–5] (better known under the commercial name "BODIPY" or difluoro*bo*ron *dipy*rromethene) have become popular fluorophores in modern materials and life science [6]. The qualities of BODIPY comprise relatively high molar absorption coefficients and fluorescence quantum yields, narrow emission bandwidths with high peak intensities, robustness towards light and chemicals, and excitation/emission wavelengths in the visible spectral region. Spectroscopic properties of BODIPY derivatives can be fine-tuned synthetically, introducing suitable substituents at positions of the difluoroboron dipyrromethene core.

*Corresponding author. Email: qinww@lzu.edu.cn

Journal of Coordination Chemistry
ISSN 0095-8972 print/ISSN 1029-0389 online
http://dx.doi.org/10.1080/00958972.2013.767896

Often, dyes are combined with material substrates to modulate properties, enhance stability, and reduce toxicity. Many multifunctional imaging and sensing dyes combine controlled material synthesis with nanofabrication [7,8]. In the last few years, researchers have taken advantage of BODIPY derivatives, modified them with diverse nanoparticles, such as Fe_3O_4 or Ni core and silica shell [9,10] or gold nanoparticles [11]. However, the spectroscopic properties and selectivity to ions between them and their corresponding BODIPY sensor have hardly changed.

In comparison with metal nanoparticles mentioned above, HA nanoparticles seem more attractive as host materials of fluorescent nanocomposites because of excellent biocompatibility and lower price. To improve the application of HA nanoparticles to biological research, fluorescent dye molecules were introduced into HA nanoparticles by using a thiourea-linkage formed in reaction of amino-terminated alkyltrialkoxysilane compounds, such as (3-aminopropyl)triethoxysilane (APTES) and dye molecules, having an isothiocyanate functional group, i.e. Fluorescein isothiocyanate [12]. The photostability and the lack of acute toxicity have become the most appreciated properties of fluorescent HA and have opened a new era of bioimaging. However, BODIPY fluorescent probes based on HA nanoparticles have not yet been reported. While there are several positions on the BODIPY chromophore which can be functionalized, suitable substituents at the third- and fifth position(s) can shift the excitation and emission bands as a function of solvent polarity/polarizability. Recently, we described that the easily obtained 3,5-dichloro-4,4-difluoro-4-bora-3a,4a-diaza-*s*-indacene derivatives can be substituted with a wide range of oxygen-, carbon-, nitrogen-, and sulfur-centered nucleophiles [13–15]. Nonsymmetrically substituted BODIPY derivatives with an *N*-substituent at the third position had wider absorption and emission bands and larger Stokes shifts than symmetric BODIPY dyes.

Bis(pyridin-2-ylmethyl)amine (commonly known as di(2-picolyl)amine, DPA) is a chelator of several metal ions. Therefore, DPA derivatives with an incorporated fluorescent moiety are attractive sensors for optical detection of metal ions [16].

In this work, we synthesize the fluorescent chemosensor **1** with 4,4-difluoro-8-(4-tolyl)-4-bora-3a,4a-diaza-*s*-indacene as fluorophore coupled at the third position to the DPA chelator and to aminated nano HA particles at the fifth position. Complex formation of **1** with Cd^{2+} or Zn^{2+} ions was studied spectroscopically.

2. Experimental

2.1. *Synthesis of BODIPY-DPA-THA nanoparticles (1)*

Dye **2** was synthesized by an efficient S_NAr reaction of **3** at room temperature [15]. This synthetic methodology is particularly valuable for obtaining symmetrically and nonsymmetrically substituted boradiazaindacene dyes with substituents at the third and fifth position(s) that are difficult to introduce otherwise. Sensor **1** was prepared in a similar S_NAr route by nucleophilic substitution of **2** with aminated nanoHA at 80 °C. The synthetic nanoparticles **1** were characterized by transmission electron microscopy (TEM), Fourier transform infrared (FTIR), UV–vis absorption and fluorescence emission spectroscopy.

2.2. *Steady-state UV–vis absorption and fluorescence spectroscopy*

UV–vis absorption spectra were recorded on a Varian UV-Cary100 spectrophotometer and for the corrected steady-state emission spectra, a Hitachi F-4500 spectrofluorometer was

employed. Freshly prepared samples in 1 cm quartz cells were used to perform all UV–vis absorption and emission measurements. For determination of fluorescence quantum yields, dilute solutions with an absorbance below 0.1 at the excitation wavelength were used. Rhodamine 6G in H_2O ($\Phi_f = 0.76$) for $\lambda_{ex} = 470$ nm was used as fluorescence standard [17]. The Φ_f values reported in this work are the averages of multiple (generally three), fully independent measurements. In all cases, correction for the solvent refractive index was applied. All spectra were recorded at 20 °C. The titration experiments were carried out by adding small quantities of a stock solution of metal perchlorates in EtOH/H_2O (95/5 V/V) to a much larger volume (10 mL) of solutions of **1**.

2.3. *Determination of K_d from direct fluorimetric titration*

The ground-state dissociation constant K_d of the complexes between Cd^{2+} or Zn^{2+} and the nanofluorescence probe were determined in EtOH/H_2O (95/5 V/V) solution by fluorometric titration as a function of Cd^{2+} or Zn^{2+} concentration using fluorescence emission spectra. Nonlinear fitting of equation (1) [18] to the steady-state fluorescence data F recorded as a function of [Cd^{2+}] or [Zn^{2+}] yields values of K_d, the fluorescence signals F_{min} and F_{max} at minimal and maximal [Cd^{2+}] or [Zn^{2+}], respectively (corresponding to the free and Cd^{2+} or Zn^{2+} bound forms of the nanofluorescence probe, respectively), and n (the number of metal ions bound per probe). Equation (1) assumes that the absorbance of the sample is small (<0.1) and that Cd^{2+} or Zn^{2+} complex formation in the excited state is negligible.

$$F = \frac{F_{max}[M^{2+}]^n + F_{min}K_d}{K_d + [M^{2+}]^n} \quad (1)$$

Fitting equation (1) to the steady-state fluorescence data F with n, K_d, F_{min}, and F_{max} as freely adjustable parameters always gave values of n close to 1 in this experiment, indicating that one Cd^{2+} or Zn^{2+} is bound per nanofluorescent indicator. Therefore, n was kept fixed at 1 in the final fittings of equation (1) to the fluorescence excitation or emission spectral data, from which the estimated values of K_d, F_{min}, and F_{max} are reported.

3. Outstanding results and discussion

3.1. *Characterization of 1*

The morphology and microstructure of THA-APTES and probe **1** nanoparticles were investigated by TEM. figure 1(a) shows the TEM image of THA-APTES nanoparticles that appear agglomerated. figure 1(b) reveals an ellipsoidal structure with a narrow size distribution (15–25 nm) of **1**, which maintained its nanocrystalline appearance.

In its infrared spectrum (figure 2), only bands of HA were observed for THA, i.e. phosphate main bands at 1036 (υ_3) cm^{-1}, 604 (υ_4), and 569 (υ_4) cm^{-1}, hydroxide bands at 3424 (υ_s) and 1637 cm^{-1} (υ_2) and carbonate bands at 1421 (υ_3) and 874 (υ_2) cm^{-1}. In addition to bands of HA, amino and –CH_2– groups of THA-APTES also give N–H bending vibration band at 1576 cm^{-1} and C–H stretching vibration at 2931 cm^{-1}. In the IR spectrum of **1**, in addition to bands attributed to THA-APTES particles themselves, strong new bands at 2965, 2859, 1302, and 1261 cm^{-1} appeared, originating from dye **2**, consistent with **2** covalently bound to THA-APTES nanoparticles [12,19,20].

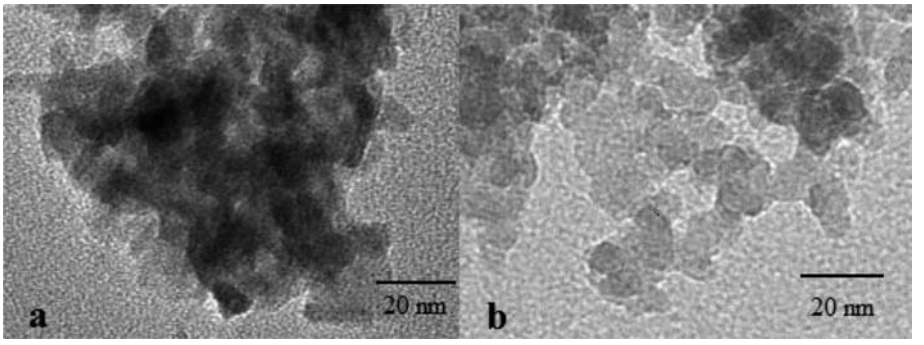

Figure 1. TEM images of (a) THA-APTES and (b) **1**.

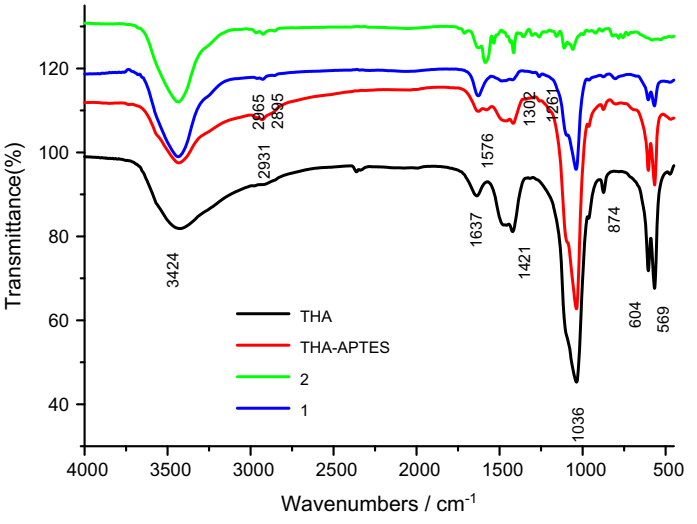

Figure 2. FTIR spectra for THA, THA-APTES, **2,** and **1**.

Figure 3 shows the normalized UV–vis absorption and fluorescence emission spectra of **1**, **2,** and **2** doped with THA or THA-APTES (without heating) dissolved in ethanol.

The absorption spectrum of **2** is of a similar shape as those of classic BODIPY dyes [21–27], with an intense absorption with a maximum λ_{abs}(max) located between 505 nm, assigned to the 0−0 band of the $S_1 \leftarrow S_0$ transition, and a shoulder (480 nm) on the high-energy side, attributed to the 0−1 vibrational of the same transition. In addition, a weaker, broad absorption – attributed to the $S_2 \leftarrow S_0$ transition – is found at 350 nm. Compound **2** exhibits typical BODIPY emission features (figure 3(b)), that is, a narrow, slightly Stokes-shifted band of mirror-image shape [18,25,26]. The maximum emission wavelength λ_{em}(max) is 556 nm. Spectroscopic measurements on **2** doped with THA or THA-APTES (without heating) were performed in an ethanol solution to provide a comparison. Compound **2** doped with THA or THA-APTES also showed an absorption at 505 nm and the corresponding emission maximum at 551 nm; there is only 5 nm difference between the wavelengths of the emission maxima λ_{em}(max) when compared with that of **2**. On the contrary, the maximum absorption wavelength λ_{abs}(max) of **1** is shifted to red in comparison

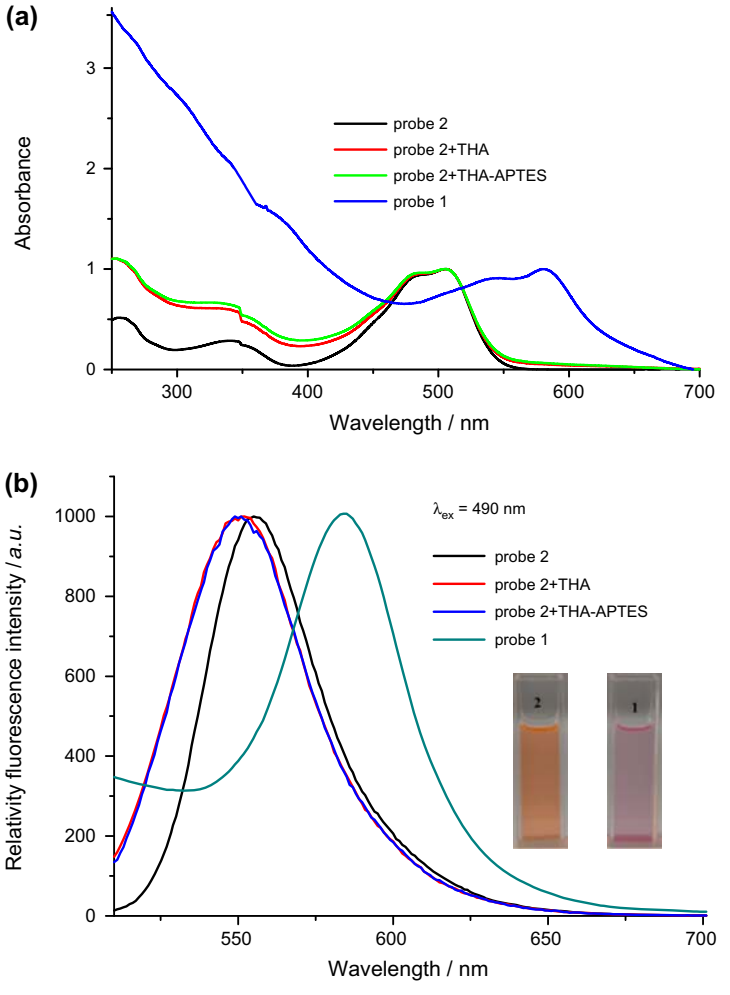

Figure 3. Normalized (a) absorbance and (b) fluorescence emission spectra (excitation at $\lambda_{ex} = 490$ nm) of **1**, **2,** and **2** doped with THA or THA-APTES (without heating) in ethanol. The inset is the image of the ethanol solution of **1** and **2** under daylight.

to dye **2**: 75 nm in ethanol (from 505 to 580 nm). Absorption spectra of **1** also show the well-known absorption pattern of common BODIPY derivatives [18,25,26]. Fluorescence emission spectra of **1** display narrow, slightly Stokes-shifted emission bands at 586 nm that are red-shifted by 30 nm compared to those of **2**.

The fluorescence quantum yield Φ_f of **1** is 0.002 in ethanol, much lower than that of **2** in ethanol (0.008). This can be understood by an influence of the substituent on BODIPY. When the electron-withdrawing group (here chlorine) was substituted by the electron-donating group (here an amino group from THA-APTES), in polar solvent, intramolecular charge transfer (ICT) from the THA-APTES amine NH to the electron-withdrawing BODIPY becomes more favored, inducing the fluorescence quenching and shifting of the spectra. The large difference in spectroscopic properties between **1** and **2** also gives us firm evidence that dye **2** has been covalently bound to the THA-APTES nanoparticles.

3.2. *Complexation of 1 with Zn^{2+} or Cd^{2+} in EtOH/H_2O (95/5 V/V)*

Di(2-picolyl)amine is a chelator of several metal ions, including Mn^{2+}, Fe^{3+}, Co^{2+}, Ni^{2+}, Cu^{2+}, Zn^{2+}, Ag^{+}, Cd^{2+}, Hg^{2+}, and Pb^{2+}.

Upon addition of Zn^{2+} or Cd^{2+} perchlorates to a solution of **2** in EtOH/H_2O (95/5 V/V), no change in the fluorescence spectra could be detected (figure S1). The selectivity is quite different even for the same chelator and fluorophore. For example, a colorimetric and NIR fluorescent turn-on BODIPY-based probe with DPA as a chelator with high selectivity for Cu^{2+} has been reported by Boens [28]. DPA was attached at the meso-position of BODIPY via a CH_2 linker to construct a detector for the selective visualization of Zn^{2+} in living cells, described by Peng and coworkers [29]. The same research group also reported a selective sensor for imaging Cd^{2+} in living cells based on ICT mechanism, built on the BODIPY platform, but with the DPA chelator attached at the third position via a *p*-styryl spacer [30].

Not only the spectroscopic properties are changed when the electron-withdrawing group was substituted by the electron-donating group, but the selectivity of **1** is also changed.

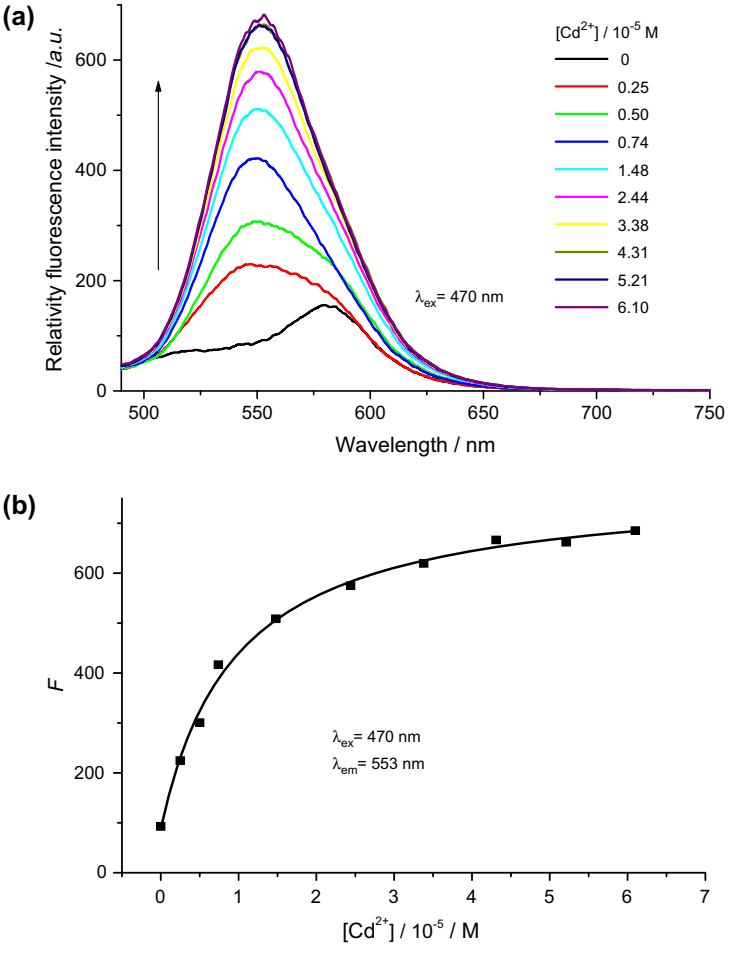

Figure 4. Fluorescence emission spectra (a) (λ_{ex} = 470 nm) of **1** (50 mg/L) in EtOH/H_2O (95/5 V/V) solution as a function of [Cd^{2+}] and (b) the best fit to the *direct* (λ_{ex} = 470 nm, λ_{em} = 553 nm) fluorimetric emission titration data (for b) of **1** as a function of [Cd^{2+}].

Contrary to **2**, Zn^{2+} or Cd^{2+} produced spectral changes of **1** in EtOH/H_2O (95/5 V/V) solution. The changes in optical properties induced by addition of Zn^{2+} or Cd^{2+} perchlorates to the EtOH/H_2O (95/5 V/V) solutions of **1** are shown in figure 4.

The lowest-energy absorption of the nanoindicator shifts hypsochromically by 70 nm (from 580 to 510 nm) when Cd^{2+} ions are added to the EtOH/H_2O (95/5 V/V) solution (figue S2(a)). The shift in the absorption spectra causes immediate change of the solution color from pink to jacinthe, which can be detected by a naked eye.

The K_d of **1** and the stoichiometry of Cd^{2+} binding were determined by changes of the absorbance as a function of Cd^{2+} concentration. The results obtained at $\lambda_{abs} = 580$ nm indicated a 1 : 1 complex stoichiometry and yielded a value of 17 ± 5 μM for K_d. Since there is a large shift of the absorption spectra, ratiometric absorption measurements could be performed. A K_d value of 8 ± 3 μM was determined by using the ratio of the increase/decrease in absorption bands at $\lambda^1_{abs}/\lambda^2_{abs} = 505/580$ nm (figure S2(b–c)).

The maximum of the fluorescence emission band shifts from 585 nm in ion-free EtOH/H_2O (95/5 V/V) to 550 nm in the presence of Cd^{2+} and is accompanied by an increase in intensity. The low $_f$ value for free **1** (0.002) can be attributed to efficient quenching via an excited-state ICT process from nitrogen of DPA to the strongly electron-deficient BODIPY acceptor. Upon binding Cd^{2+}, the electron-donating properties of the amine of DPA are reduced, partially suppressing the ICT and causing an enhancement in the fluorescence quantum yield. The highest fluorescence quantum yield value (0.01 for excitation at 470 nm) is found above 43 μM Cd^{2+} in EtOH/H_2O (95/5 V/V) solution.

The K_d value of 9.6 ± 1.0 μM for the Cd^{2+} complex with **1** was obtained from direct fluorimetric titrations (equation 1) using emission spectra. The titration indicated a well-defined 1 : 1 stoichiometry between **1** and Cd^{2+}.

The spectral changes observed when Zn^{2+} was added into the EtOH/H_2O (95/5 V/V) solution of **1** are very similar to those for Cd^{2+} (figure S3). Usually discrimination between Cd^{2+} and Zn^{2+} is very difficult because they are stereoelectronic isosteres. The highest

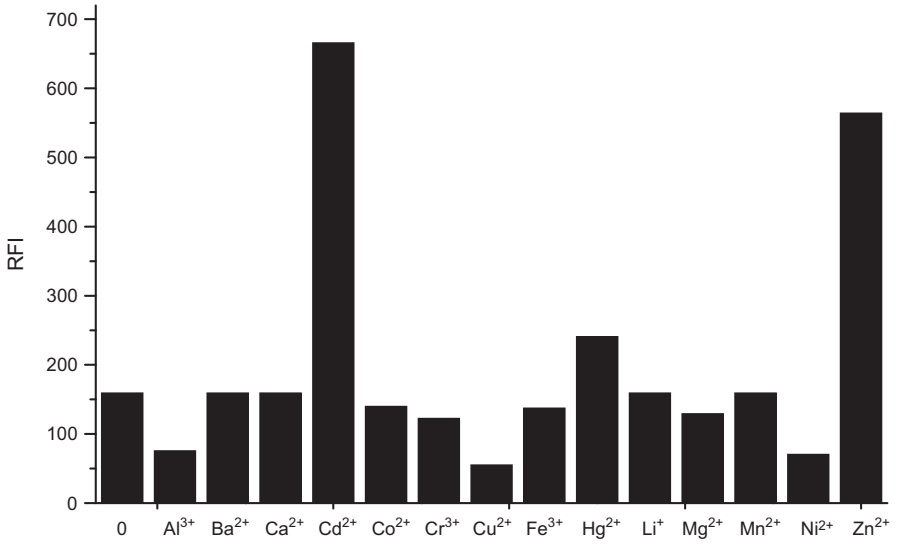

Figure 5. Fluorescence intensity of the solution of **1** (50 mg/L) in EtOH/H_2O (95/5 V/V) after addition of 0.2 μmol of various cations.

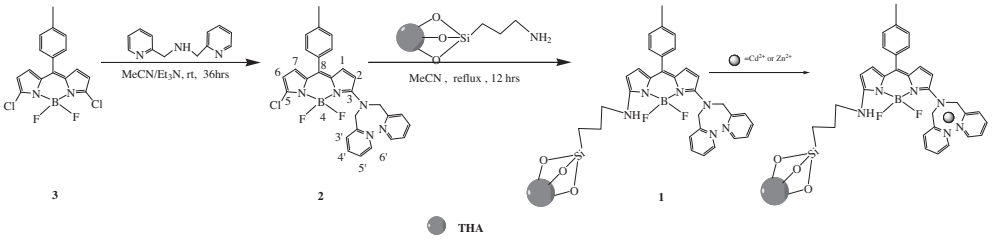

Scheme 1. Synthesis of BODIPY-functionalized THA nanoparticle **1**.

fluorescence quantum yield value (0.01 for excitation at 470 nm) is found above 83 μM Zn^{2+} in EtOH/H_2O (95/5 V/V) solution. A K_d value of 39 ± 4 μM was obtained for 1 : 1 complex with Zn^{2+} by direct fluorimetric titration.

The changes of optical properties of **1** have also been observed on addition of Zn^{2+} or Cd^{2+} nitrates (other counter anion salt), as well as with the corresponding perchlorates, both giving very similar results (figures S4 and S5).

Achieving selectivity for the analyte of interest over a complex background of potentially competing species is a challenging task in sensor development. figure 5 illustrates the fluorescence response of **1** in the presence of some metal ions. Since the emission intensity of **1** almost does not change on addition of other metal ions, detection of Zn^{2+} or Cd^{2+} by **1** is hardly affected by these common coexistent metal ions Scheme 1.

We compare BODIPY-DPA-THA nanoparticles (**1**) with representative literature values for some BODIPY nanofluorescent probes mentioned above [9–11]. The spectroscopic properties and selectivity to ions between BODIPY–Fe_3O_4 or Ni or gold nanoparticles and their corresponding BODIPY sensor hardly changed. In *contrast*, the absorption and emission maxima of nanoparticles **1** in ethanol are red-shifted in comparison to the corresponding BODIPY dye **2**; the selectivity of **1** has also been changed in comparison to **2**.

4. Conclusions

We have synthesized a new fluorescent chemosensor BODIPY-DPA-THA (**1**) by nucleophilic substitution of fluorescent dye **2** with nanoparticles THA. Unlike literature values for BODIPY–Fe_3O_4 or Ni or gold nanoparticles and their corresponding BODIPY sensors, there is quite a large difference in the properties between dye **2** and nanofluorescent chemosensor **1**. The absorption and emission maxima of **1** in ethanol are red-shifted by 75 and 30 nm, respectively, in comparison to **2**. Compound **1** can form 1 : 1 complexes with Cd^{2+} or Zn^{2+} ions in EtOH/H_2O (95/5 V/V) solutions, producing a color change along with large *hypsochromic* shifts in the absorption and fluorescence spectra. On the contrary, the fluorescence spectrum of **2** is unchanged in the presence of Cd^{2+} or Zn^{2+}.

Acknowledgment

This work was supported by the Chinese "Program for New Century Excellent Talents in University" (NCET-09-0444), the "Fundamental Research Funds for the Central Universities" (lzujbky-2011-22 and lzujbky-2012-k13), the National Science Foundation for Fostering Talents in Basic Research of the National Natural Science Foundation of

China (Grant No. J1103307) and the "International Cooperation Program of Gansu Province" (1104WCGA182). The authors would like to thank the Natural Science Foundation of China (No. 21271094), and this study was supported in part by the "Key Program of National Natural Science Foundation of China" (20931003).

References

[1] B. Biswas, S.P. Hung, H.L. Tsai, R. Ghosh, N. Kole. *J. Coord. Chem.*, **65**, 2280 (2012).
[2] J.P. Desvergne, A.W. Czarnik (Eds.). *Chemosensors of Ion and Molecule Recognition*, Kluwer, Dordrecht (1997).
[3] R. Ziessel, G. Ulrich, A. Harriman. *New J. Chem.*, **31**, 496 (2007).
[4] A. Loudet, K. Burgess. *Chem. Rev.*, **107**, 48912 (2007).
[5] G. Ulrich, R. Ziessel, A. Harriman. *Angew. Chem. Int. Ed.*, **47**, 1184 (2008).
[6] R.P. Haugland, *The Handbook. A Guide to Fluorescent Probes and Labeling Technologies*, 10th Edn, Molecular Probes Inc., Eugene, OR (2005).
[7] G.M. Whitesides. *Small*, **1**, 172 (2005).
[8] O.C. Farokhzad, R. Langer. *Adv. Drug Delivery Rev.*, **58**, 1456 (2006).
[9] H. Son, H.Y. Lee, J.L. Lim, D. Kang, W.S. Han, S.S. Lee, J.H. Jung. *Chem. Eur. J.*, 16, 11549 (2010).
[10] H.Y. Lee, D.R. Bae, J.C. Park, H. Song, W.S. Han, J.H. Jung. *Angew. Chem., Int. Ed.*, **48**, 1239 (2009).
[11] H.Y. Lee, H. Son, J.L. Lim, J. Oh, D. Kang, W.S. Han, J.H. Jung. *Analyst*, **135**, 2022 (2010).
[12] H.Y. Liu, F.J. Chen, Z.Z. Zeng. *J. Phys. Chem. C*, **115**, 18538 (2011).
[13] M. Baruah, W.W. Qin, N. Basarić, W.M. De Borggraeve, N. Boens. *J. Org. Chem.*, **70**, 4152 (2005).
[14] M. Baruah, W.W. Qin, R.A.L. Vallée, D. Beljonne, T. Rohand, W. Dehaen, N. Boens. *Org. Lett.*, **7**, 4377 (2005).
[15] T. Rohand, M. Baruah, W.W. Qin, N. Boens, W. Dehaen. *Chem. Commun.*, **266**, (2006).
[16] K. Kyose, H. Kojima, Y. Urano, T. Nagano. *J. Am. Chem. Soc.*, **128**, 6548 (2006).
[17] J. Olmsted. *J. Phys. Chem.*, **83**, 2581 (1979).
[18] E. Cielen, A. Tahri, K. Ver Heyen, G.J. Hoornaert, F.C. De Schryver, N. Boens. *J. Chem. Soc., Perkin Trans.*, **2**, 1573 (1998).
[19] Y. Zhang, J.L. Cryst. *Growth Des.*, **8**, 2101 (2008).
[20] M. Markovıc, B.O. Flower, M.S. Tung. *J. Res. Natl. Inst. Stand. Technol.*, **109**, 553 (2004).
[21] K. Rurack, M. Kollmannsberger. *J. Angew. Chem. Int. Ed.*, **40**, 385 (2001).
[22] E. Vos de Wael, J.A. Pardoen, J.A. van Koeveringe, J. Lugtenburg. *Recl. Trav. Chim. Pays-Bas*, **96**, 306 (1977).
[23] K. Rurack, M. Kollmannsberger. *New J. Chem.*, **25**, 289 (2001).
[24] A. Coskun, E.U. Akkaya. *J. Am. Chem. Soc.*, **127**, 10464 (2005).
[25] M. Baruah, W.W. Qin, C. Flors, J. Hofkens, R.A.L. Vallée, D. Beljonne, M. Van der Auweraer, W.M. De Borggraeve, N. Boens. *J. Chem. Phys. A*, **110**, 5998 (2006).
[26] T. López Arbeloa, F. López Arbeloa, I. López Arbeloa, I. García-Moreno, A. Costela, R. Sastre, F. Amat-Guerri. *Chem. Phys. Lett.*, **299**, 315 (1999).
[27] A. Costela, I. García-Moreno, C. Gomez, R. Sastre, F. Amat-Guerri, M. Liras, F. López Arbeloa, J. Bañuelos Prieto, I. López Arbeloa. *J. Phys. Chem. A*, **106**, 7736 (2002).
[28] S. Yin, V. Leen, S. Van Snick, N. Boens, W. Dehaen. *Chem. Commun.*, **46**, 6329 (2010).
[29] Y. Wu, X.J. Peng, B. Guo, J. Fan, Z. Zhang, J. Wang, A. Cui, Y. Gao. *Org. Biomol. Chem.*, **3**, 1387 (2005).
[30] X. Peng, J. Du, J. Fan, J. Wang, Y. Wu, J. Zhao, S. Sun, T. Xu. *J. Am. Chem. Soc.*, **129**, 1500 (2007).